Thoroughly Hydrophilized Electrospun Poly(*L*-Lactide)/Poly(ε-Caprolactone) Sponges for Tissue Engineering Application

Chengzhang Xu, Jun Young Cheong, Xiumei Mo, Valérie Jérôme, Ruth Freitag, Seema Agarwal, Reza Gharibi,* and Andreas Greiner*

Biodegradable electrospun sponges are of interest for various applications including tissue engineering, drug release, dental therapy, plant protection, and plant fertilization. Biodegradable electrospun poly(l-lactide)/poly(ε-caprolactone) (PLLA/PCL) blend fiber-based sponge with hierarchical pore structure is inherently hydrophobic, which is disadvantageous for application in tissue engineering, fertilization, and drug delivery. Contact angles and model studies for staining with a hydrophilic dye for untreated, plasma-treated, and surfactant-treated PLLA/PCL sponges are reported. Thorough hydrophilization of PLLA/PCL sponges is found only with surfactant-treated sponges. The MTT assay on the leachates from the sponges does not indicate any cell incompatibility. Furthermore, the cell proliferation and penetration of the hydrophilized sponges are verified by in vitro cell culture studies using MG63 and human fibroblast cells.

1. Introduction

Water insoluble biodegradable polymers are of utmost importance in several application fields, such as tissue engineering,[1,2] gene delivery,[3,4] drug delivery,[5,6] and agriculture.[7,8] Furthermore, biodegradable polymers have gained relevance for microplastic debris.[9–11] Prominent examples of water-insoluble biodegradable polymers are aliphatic polyesters, such as poly (L-lactide) (PLLA), polycaprolactone (PCL), polyglycolide, polyhydroxyalkanoates and their copolymers.[12,13] Among biodegradable polyesters, PLLA and its copolymers are frequently used in different biomedical applications like implants, scaffolds for tissue engineering, and as drug-release carriers. The inherent surface hydrophobicity of these polyesters is a drawback in, e.g., tissue engineering since hydrophobic surfaces do not bind proteins.[14] In contrast, a hydrophilic surface promotes cell adhesion and mass transfer of nutrition and metabolism products, which results in cell proliferation.[15]

Numerous efforts have been reported in the literature to tune the surface wetting properties of PLLA by alkaline treatment,[16] coating with hydrophilic materials, such as type-I collagen[17] and chitosan,[18] oxygen, and ammonia plasma treatment.[19,20] The need for surface modification of PLLA is already described well by reviews.[21,22] In previous study, hydrophilicity of biodegradable polyester was increased by plasma treatment on poly(lactic-*co*-glycolic acid) (PLGA) film.[19] After plasma treatment, high

C. Xu, S. Agarwal, A. Greiner
Macromolecular Chemistry and Bavarian Polymer Institute
University of Bayreuth
Universitätsstrasse 30, 95440 Bayreuth, Germany
E-mail: greiner@uni-bayreuth.de

J. Y. Cheong
Bavarian Center for Battery Technology (BayBatt) and Department of Chemistry
University of Bayreuth
Universitätsstrasse 30, 95440 Bayreuth, Germany

X. Mo
State Key Laboratory for Modification of Chemical Fibers and Polymer Materials
College of Biological Science and Medical Engineering,
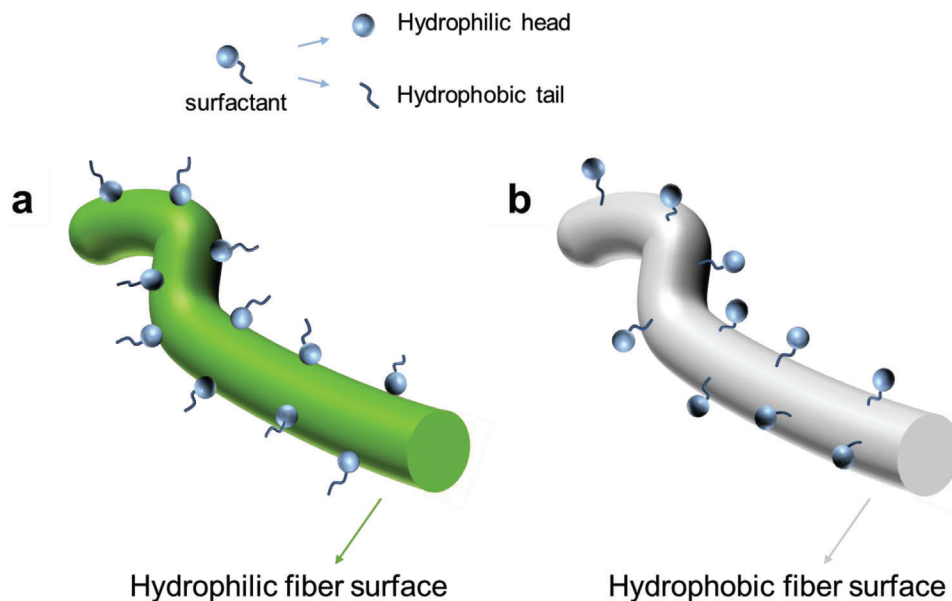Donghua University
Shanghai 201620, P. R. China

V. Jérôme, R. Freitag
Chair for Process Biotechnology
University of Bayreuth
Universitätsstrasse 30, 95440 Bayreuth, Germany

R. Gharibi
Department of Organic Chemistry and Polymer, Faculty of Chemistry
Kharazmi University
Tehran 15719-14911, Iran
E-mail: r.gharibi@khu.ac.ir

Scheme 1. Hydrophilic and hydrophobic fiber surface modified by surfactant a) hydrophilic surface modified by surfactant and b) hydrophobic surface modified by surfactant.

quantities of hydroxyl and peroxyl groups were detected from PLGA film. Another kind of agent, surfactants, which in general can change the wetting properties of the polymer films and particles,[23] are also used for surface modification in recent research. In one of the studies, poly(*D, L*-lactic acid)-*block*-poly(ethylene glycol) particles were coated with surfactant Tween 80 to increase the surface hydrophilicity and the stability, strength and the capacity to penetrate blood–brain barrier of drug-loaded particles.[24]

In some applications, porous structure of polymeric three-dimensional (3D) scaffold is profitable. For example, in the field of tissue engineering, porous structure of material is expected to facilitate cell seeding and proliferation. Additionally, blood vessels invade, thus, to supply enough nutrition and have an efficient mass transfer.[25] Therefore, the porosity of artificial scaffolds for tissue engineering is of importance. Different techniques such as porogene leaching,[26,27] gas foaming,[28] phase separation,[29] and 3D printing[30] have been performed to fabricate scaffolds with porous structure. Recently, a new method combining electrospinning and self-assembly was shown to fabricate low-density 3D open cellular scaffold with hierarchical pore size to mimic natural sponge structure. These scaffolds are named as electrospun sponges. The pores of these sponges with a range of size from 10–400 μm are formed by sublimation of the solvent during freeze-drying step and mechanical stability is realized by self-assembly of electrospun short fibers.[31–34] Following this concept electrospun sponges made of biodegradable polymers, including poly(L-lactide) (PLLA), were reported in recent literature as they are of interest for tissue engineering.[35–41] For example, Chen et al. produced PLLA/gelatin fiber-based sponge with cytocompatibility, which is suitable for cartilage tissue engineering. The hydrophilicity of these sponges was tuned by the addition of gelatin.[35,36] Xu et al. developed a new method (thermally induced self-agglomeration) to fabricate PCL and PCL/PLLA sponges.[37,38] The hydrophilicity of these sponges was achieved

by the application of gelatin in short fiber dispersion medium. Miszuk et al. used hydroxyapatite coated PCL sponge for bone tissue regeneration, and in vitro study showed that osteogenic differentiation of cells was improved on the sponge.[39] Recently, we showed the use of PLLA/PCL short fibers to fabricate sponges, in which the self-assembly is achieved by physical cross-linking of PCL with low melting point.[40] The compatibility of these sponges to Jurkat cells and their proliferation worked well but the penetration of the cells into the sponge was limited. The hydrophilization of the sponges was improved by coating with an amphiphilic carbohydrate block copolymer, which resulted in more homogenous cell seeding and proliferation in a perfusion reactor.[41]

Recently, intrinsically hydrophobic polyimide (PI) sponges were hydrophilized by use of the surfactant sodium dodecyl benzenesulfonate (SDBS). PI short electrospun fibers were dispersed in an aqueous solution of SDBS. After freeze drying the PI sponges showed hydrophilic properties on the surface and fast water absorption.[42] The concept of surface wettability of hydrophilic as well as hydrophobic fibers is schematically depicted in **Scheme 1**. While hydrophilic fibers should become hydrophobic by treatment with surfactants, hydrophobic fibers become hydrophilic, which has been applied for two-dimensional (2D electrospun nonwoven for hydrophilization.[43,44] The use of surfactants for the hydrophilization of fibrous scaffolds provides a straightforward and highly efficient approach to achieve a high degree of hydrophilization. Particular advantage of surfactant is the high mass transfer with fibrous scaffold. This advantage of surfactants for the hydrophilization of fibrous scaffolds could be translated to 3D biodegradable PLLA sponges, and thereby could be of advanced interest for PLLA sponges for cartilage, bone tissue, and liver tissue engineering. However, it is crucial to prove the thorough hydrophilization of the PLLA sponges and the cell compatibility for practical use in tissue engineering applications. Therefore, we explored the hydrophilization of PLLA/PCL

**ADVANCED
SCIENCE NEWS**

www.advancedsciencenews.com

[M] acro-
molecular
Bioscience

www.mbs-journal.de

Table 1. Details of PFSs used in this work.

PFS	PFS-1	PFS-2	PFS-3
density [mg cm^{-3}]	153	80	54
porosity[a] [%]	87	93	96

[a] calculated based on Equations S1 and S2

sponges by use of the surfactant Tween 20, which has a relatively low LD$_{50}$ value (LD$_{50}$ of SDBS: 2.3 mg L^{-1} (given for fish, data for human cells are not published to the best of our knowledge),[45] LD$_{50}$ of Tween 20: 40 554 mg kg^{-1}).[46] We verified the cell compatibility of the hydrophilized sponges by cell tests with human fibroblast and MG63 cells. The cell tests applied to the sponges are based on our previous evaluation of cell response.[47–50] In contrast to hydrophobic sponges, excellent cell adhesion and cell proliferation were proven for the hydrophilized sponges. However, these sponges could also be of interest for other applications, e.g., dental implant, fertilization, and plant protection. The potential application in agriculture field attributes to its hydrophilicity, thus, it has the possibility to serve as a water reservoir. Besides the importance of hydrophilization of sponges for tissue engineering, it is also of major interest to investigate the cell response to hydrophilized fibrous objects like sponges as it mimics to some

extent textile scaffold waste in the environment and address this topic of microplastic debris as well.[51] The result of cell test on sponges will help in understanding the impact of short fibers from textile to organisms, which is important to microplastic.

2. Result and Discussion

2.1. Sponge Preparation and Hydrophilization

PLLA/PCL (9:1 w/w) blend electrospun nonwoven fibers were used to prepare 3D porous polymer fiber-based sponges (PFSs). PFSs were prepared with different densities and porosities, which are shown in **Table 1** and Table S1 (Supporting Information) (PFSs 4–7). The process of PFSs preparation is illustrated in **Figure 1**a. The PFSs preparation was done in three steps: electrospinning of the nonwoven (step A), cutting of the nonwoven for the preparation of short fibers (step B), and dispersion of the short fibers followed by freeze-drying (step C). In detail, the as-spun PLLA/PCL nonwoven (morphology shown in Figure 1b, fiber diameter at the range of 0.8 – 1 μm) were first cut to short fibers (fiber length 50–150 μm) in water/ice. Homogenization of the resulting short fiber dispersion was achieved by addition of different amount of Tween 20 (0.01 wt.% or 1 wt.%, **Table 2**), which was essential for the preparation of homogeneous PFSs (Figure 1c). In the case of the sponge with lower density, 0.01%
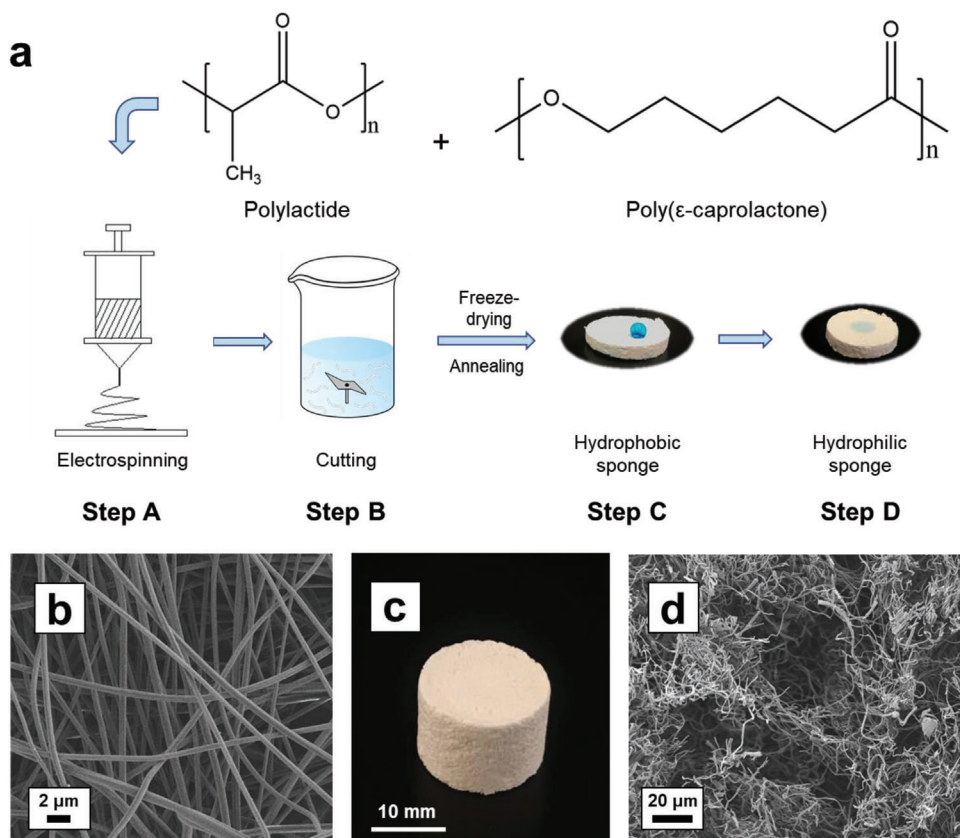
Figure 1. a) Schematic illustration of PFS preparation process of PFS (step A: electrospinning of PLLA/PCL blend; step B: cutting nonwoven and dispersing of short fiber; step C: freeze-drying and thermal cross-linking of sponge; step D: dip-coating of sponges in Tween 20 or plasma treatment). b) Morphology of PLLA-PCL as-spun nonwoven. c) Macroscopic appearances of PFS-3 and d) morphology of PFS-3 (scanning electron microscope micrograph).

**ADVANCED
SCIENCE NEWS**

www.advancedsciencenews.com

Macromolecular
Bioscience

www.mbs-journal.de

Table 2. Details of Tween 20 treated PFSs.

PFS	Tween 20 concentration at step B[a] [%]	Tween 20 concentration at step D[b] [%]	Plasma treatment
PFS-1	1	0	No
D-PFS-2	0.01	1	No
D-PFS-3	0.01	1	No
P-PFS-3	0.01	0	Yes

[a] concentration of Tween 20 used to disperse short fibers (step B in Figure 1a);
[b] concentration of Tween 20 used in dip-coating step (step D in Figure 1a).

Tween 20 aqueous solution was added into the short fiber suspension to reach a lower concentration of the short fibers. Contrarily, for higher density sponges, more of the dispersion medium, 0.01% Tween 20 aqueous solution was removed by filtration to get a higher concentration of the short fibers. In contrast, PFSs prepared in aqueous suspension without Tween 20 were inhomogeneous (Figure S1, Supporting Information). Subsequently, the water was removed by freeze-drying at −70 °C. The resulting PFS were bonded by annealing at 60 °C, which is the melting temperature of PCL (Figure S2, Supporting Information) but does not melt PLLA (Figure S3, Supporting Information). At this temperature, PCL melted and formed physical cross-links between the fibers. PCL was chosen due to its rather low melting point, thus, it worked as glue to bind the short fibers together at the annealing temperature. Without the existence of PCL, the pure PLLA fiber had to be annealed at a rather high temperature for a much longer time to maintain the mechanical stability of the sponge. Contrarily, if the PCL content was too high, due to the low melting point, the sponge shrank a lot during the annealing.[40] For hydrophilization of the PFSs, step D was applied: either dip-coating of sponge in 1 wt.% Tween 20 solution or plasma treatment. The sponges treated according to step D are defined as D-PFS-X, whereas is X the specific number of the PFS sample. PFSs were successfully prepared with a density ranging from 54 to 153 mg cm⁻³. SEM measurements demonstrated the porous structure of PFSs. (Figure 1c,d). We have selected PFS-3 for most of the further experiments, because it could be handled well while the porosity is relatively high. PFS-3 in Figure 1d has the porosity of 96% (detail of calculation as Equations S1 and S2, Supporting Information) The pore size of PFS-3 ranged from 20 -160 µm (Figure S4, Supporting Information).

As discussed in detail below, all the as-prepared PFSs which were dispersed in 0.01 wt.% Tween 20 at step B are hydrophobic and require hydrophilization for cell applications. The PFSs were hydrophilized either by dispersion of short fiber in high concentration (1 wt.%) Tween 20 (in step B of Figure 1a), dip-coating of PFSs in Tween 20 (step D), or plasma treatment.

The hydrophobicity/hydrophilicity of the PFSs was analyzed by contact angle measurement on the PFSs' surface and in the middle of the cross-section. PFS-1 prepared from the highest Tween 20 concentration (1%) showed immediate water uptake and thereby high hydrophilicity (Figure S5a, Supporting Information). That result implied, that if the sponge was prepared with a high concentration of Tween 20 (1 wt.%) in step B, the sponge was hydrophilic originally. However, this sponge with high concentration of Tween from step B resulted in obvious shrinkage

and the shape of the sponge is irregular (Figure S5b, Supporting Information). Thus, sponge with lower amount of Tween from step B is essential. We analyzed the contact angles of PFS-2 and found the contact angle to be ≈138 ° on the surface and cross-section (**Figure 2**a,b). Although shrinkage was observed to some extent (≈15%) for all PFSs, it was extreme for PFS-1. Therefore, hydrophilization was applied by dip-coating of PFS-3 (here the fiber suspension for sponge preparation (Figure 1a step B) contained only 0.01 wt.% Tween 20) into 1% Tween solution (D-PFS-3). D-PFS-3 takes up water in less than 0.2 seconds according to the video of the contact angle camera, Figure 2c. Due to its immediate water uptake, D-PFS-3 is obviously highly hydrophilic. As a benchmark, we have also analyzed plasma-treated PFS-3 (P-PFS-3) according to a previously published method.[40] The thorough hydrophilization by dip-coating with Tween 20 was demonstrated for D-PFS-3 by dying with an aqueous solution of the hydrophilic dye Wussita blau.[52] After cutting from the middle vertically, the Wusitta blau was found thoroughly distributed all over the cross-section of the D-PFS-3 (**Figure 3**a). In contrast, the untreated PFS (PFS-3, without either dip-coating or plasma treatment in step D) and the plasma-treated sponge P-PFS-3 only absorbed Wusitta blau on its surface (Figure 3a). The hydrophilicity of D-PFS was further verified by dipping the hydrophobic PFS-3 and hydrophilic D-PFS-3 together in water. D-PFS-3 sinks in water within several seconds, whereas the PFS-3 was floating on the surface of water (Figure 3b). D-PFS-3 sinks into water because the water could penetrate the sponges, implying the hydrophilicity of D-PFS-3.

2.2. Cytotoxicity Evaluation

Because of the potential application of the prepared sponges for tissue engineering and biomedical application purposes, the absence of leaking substances with toxic effects is essential. To this aim, the possibility of leaking toxic substances from the designed scaffolds was examined by performing the MTT assay after 24 h on MG63 and HDF fibroblast cells cultivated in the growth medium containing the extracted leachates obtained from soaked PFS samples in the culture medium. The model study by hydrophilic dye already verified, that the Wusitta blau could not penetrate the plasma-treated sponge (P-PFS-3). The result indicates that the cell culture medium, which is also aqueous, will not penetrate the sponge either to allow cell infiltration. The high viability of cultured MG63 and HDF cells in the presence of the specific amount of extracted leachates of samples (over 95%) and no significant reduction after 24 h compared to the negative control confirmed the nontoxicity of the extracted leachates (**Figure 4**a,b). For further confirmation, the cell viability was followed at a more extended time on extracted leachates with HDF cells until 10 days. The result showed the viability of cells remained above 90% for one-week extraction, and even after ten days of extraction, only a slight decrease in cell viability was detected (Figure 4c). Therefore, we could conclude that there is no release of toxic material or the released material are lower than the toxicity level, which is another indication of the suitable integration of Tween 20 within the polymeric fiber of PFS's structure. It is worth mentioning that at 24 h, the HDF cell viability on D-PFS-3 leachate is higher. However, at the latter recording points
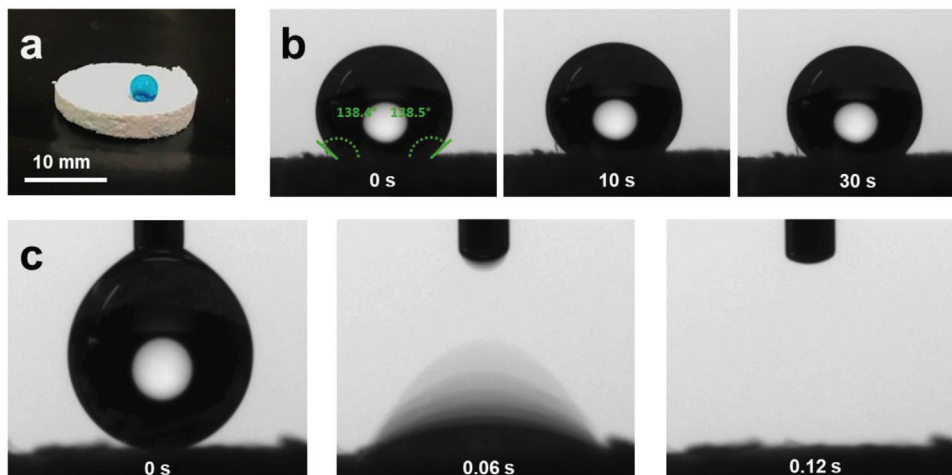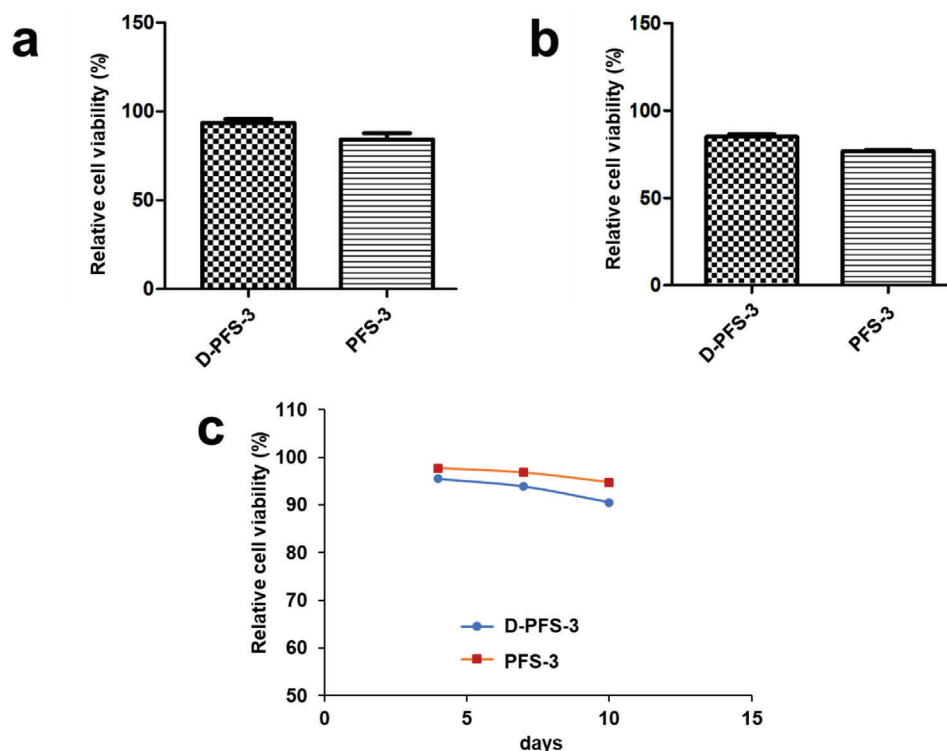
Figure 2. a) Image of liquid uptake by PFS-2 (dyed by Wusitta blau). Photographic image of contact angle measurements b) PFS-2 and c) D-PFS-2.
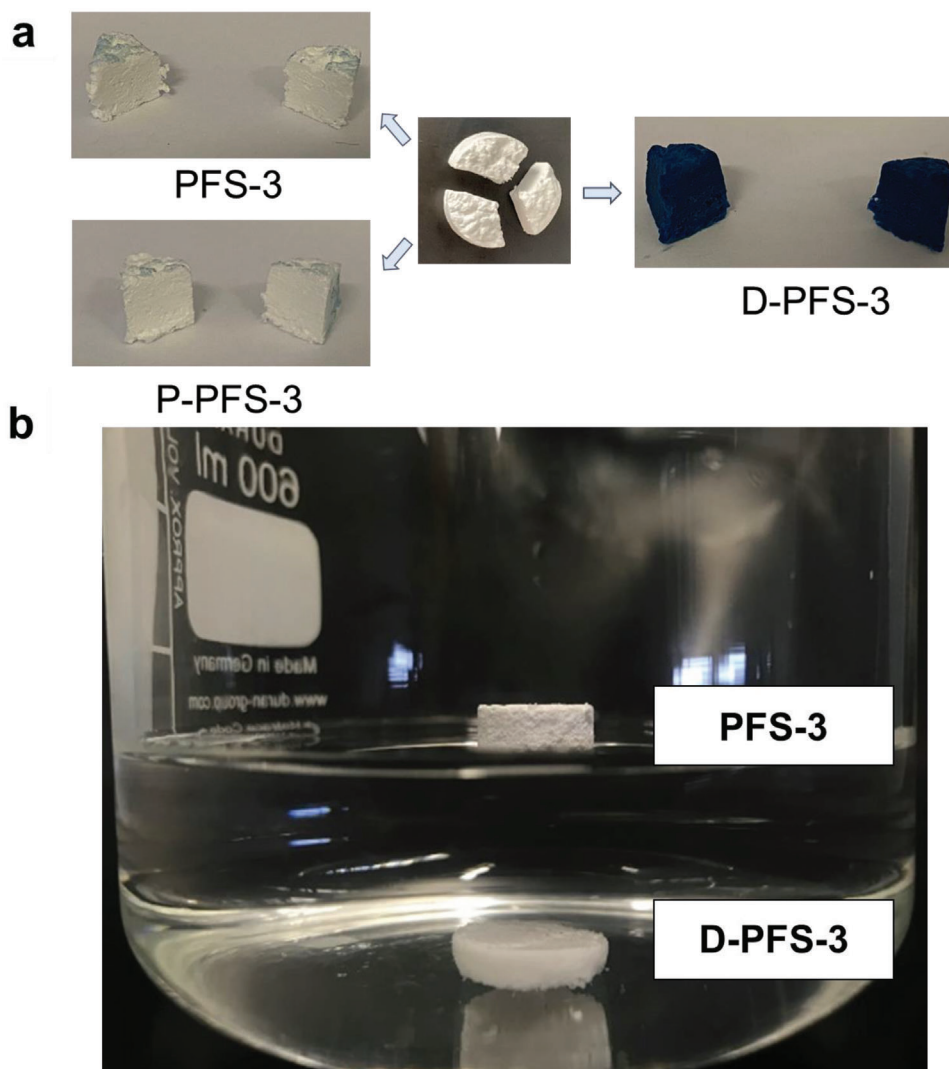
Figure 3. a) Cross section of PFS-3 (left) and P-PFS-3 (center) and D-PFS-3 (right) after immersing in hydrophilic dye (Wusitta blau) for 30 min. b) D-PFS-3 (submerged) and PFS-3 (floating) in deionized water.

Figure 4. a) The cytotoxicity analysis of MG63 cells on leachate extracted from the D-PFS-3 and PFS-3 after 24 h. b) The cytotoxicity analysis of HDF cells on leachate extracted from the D-PFS-3 and PFS-3 after 24 h (Control: cell culture plate = 100% cell viability). c) HDF cell viability monitoring on leachate extracted from the D-PFS-3 and PFS-3 over 10 days.

(96, 168, and 240 h), the HDF cell viability on PFS-3 is higher. The assumption is the HDF cell viability changed slightly between the two recording points (24 and 96 h), which was not further studied. It should be noted at this point, that the PFS did not show any macroscopic morphological changes during the test period for cytotoxicity study (10 days).
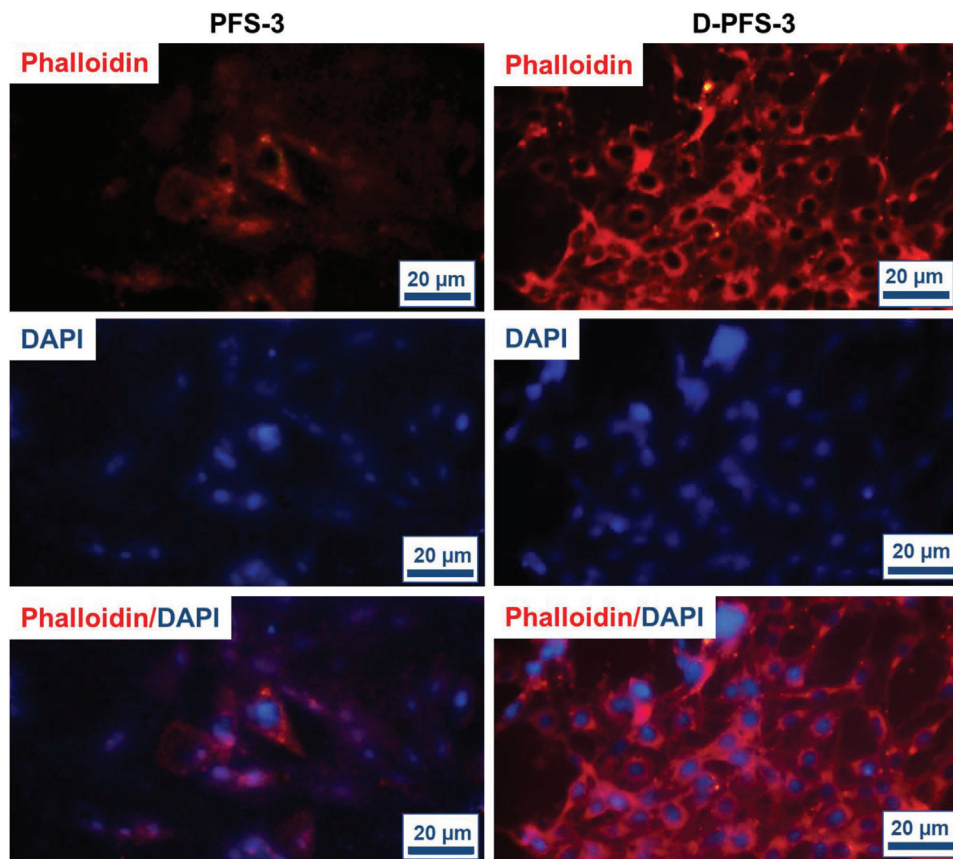
2.3. Cell Adhesion Study

The absorption and adhesion of cells on the surface of scaffolds have a vital role in the growth and proliferation of cells and, finally, the formation of tissue within the scaffold structure. The effect of surface chemistry, especially hydrophilicity, and hydrophobicity of PFS surface on the biomolecules, protein, and cell adhesion and proliferation, has also been established in previous research.[45–48] The adhesion of MG63 and HDF cells lines (these two cell lines were used to evaluate the potential application of scaffolds for both bone and skin regeneration application) on both D-PFS-3 (hydrophilic) and PFS-3 (hydrophobic) scaffolds was assessed in the present study. The quantitative adhesion result was calculated using cell culture well plate as negative control. The quantified number is shown in **Figure 5**, the morphology, and population of the adhered MG63 and HDF cells on the scaffolds are shown in **Figure 6**, and **Figure 7**. As can be seen in Figure 5, the population of both MG63 and HDF cells on the D-PFS-3 sample is significantly higher than that on the hydrophobic PFS-3 scaffold, and only a few adhered cells were noticed on
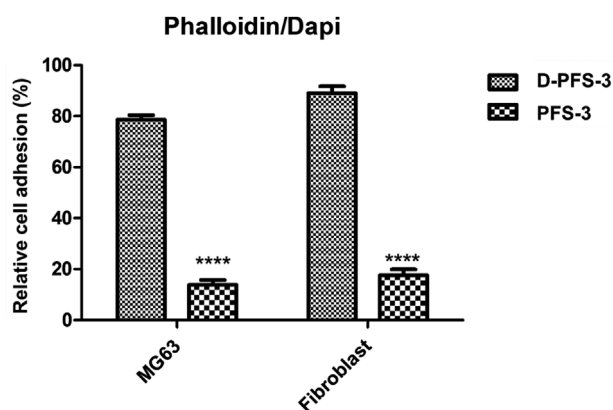
Figure 5. The relative adhesion of MG63 and HDF cells on PFS-3 and D-PFS-3 samples (****: p value<0.0001, unpaired t test, two tailed p value).

PFS-3 scaffold. The relative cell adhesion of ≈80% and 92% for MG63 and HDF cells was recorded for the D-PFS-3 sample. In contrast, the relative cell adhesion on the PFS-3 decreased and reached lower than 20% for both cell lines. It is worth noticing that even within the significant drop in relative adhesion of cells on the PFS-3 scaffold, the relatively adhered cells remained viable with spindle-shaped morphology up to 48 h, which confirmed its non-toxicity behavior. The previous reports have shown that the hydrophobic nature of pure PLLA and PCL limits the adhesion and proliferation of cell. The same trend was recorded

**ADVANCED
SCIENCE NEWS**

www.advancedsciencenews.com

**[M] acro-olecular
Bioscience**

www.mbs-journal.de

Figure 6. Morphology of stained proliferated MG63 cells on scaffolds. Cell nuclei were stained with DAPI, F-actin stained with Alexa Fluor® 488-phalloidin.

for the hydrophobic scaffold in the present study (Figure 6 and Figure 7). The remarkable relative adhesion, growth, and proliferation of both MG63 and HDF on D-PFS-3 scaffolds are attributed to its suitable hydrophilicity that leads to high protein binding to biomolecules, and higher relative cell adhesion. This result verifies that incorporating the Tween 20 within PLLA/PCL scaffold is a promising approach to overcome the limitations mentioned earlier, leading to superior cellular interaction and adhesion. The excellent relative cell adhesion and proliferation of both MG63 and HDF on hydrophilic scaffolds imply their potential application for both skin and bone tissue regeneration.

### 2.4. Penetration and Growth of Cells Within PFSs

Limitations of cell and biomolecule penetration into the scaffolds led to formation of mature tissue on the outer layer and necrotic tissue in the center of scaffolds. The infiltration of cells inside the sponge also relies on the pore structure and pore size of the sponge. To address these issues, designing of porous scaffolds with superior ability to transfer nutrient and cell into their inner layer has prime importance. The penetration of both HDF and MG63 cells into the prepared PFSs was also examined in the present work. To this aim, the cells were seeded onto the PFSs' surfaces, and then the viability, extent and depth of cell growth and penetration were followed by staining of penetrated

and grown cells. The images of transverse sections of the cell-seeded PFSs after H&E staining after two days are shown in **Figure 8**a,b. Depth of penetration into the scaffolds was quantified after 48 h. No significant cell penetration was detected for the hydrophobic PFS-3 for both cell lines after 48 h. In contrast, proper number cell/tissue penetration into the middle of the D-PFS-3 was observed. The cell penetration depth of 211 ± 22 and 384 ± 53 μm was recorded for MG63 and HDF cell lines after 48 h, respectively. The observed difference between the depth and extent of cell growth for two different cell lines could be related to the dimensions of cells and hydrophilicity of the seeded cell types. The cells were also properly spread on the edge and surface of D-PFS-3 scaffold. The recorded result proved that the developed scaffolds with tuned hydrophilicity could support tissue formation throughout either surface, edge, or middle of constructed scaffold. Based on recorded results we could conclude that the prepared scaffolds from both physical and biological point of view are properly designed and are enabled to support cell activity and let the cell proliferate. The successful infiltration of the cells in the sponge also indicated that the pore size was suitable for cell penetration.

3. Conclusion

Polymer fiber-based PFS was fabricated successfully from the blend polymer system PLLA/PCL. During the cutting process,
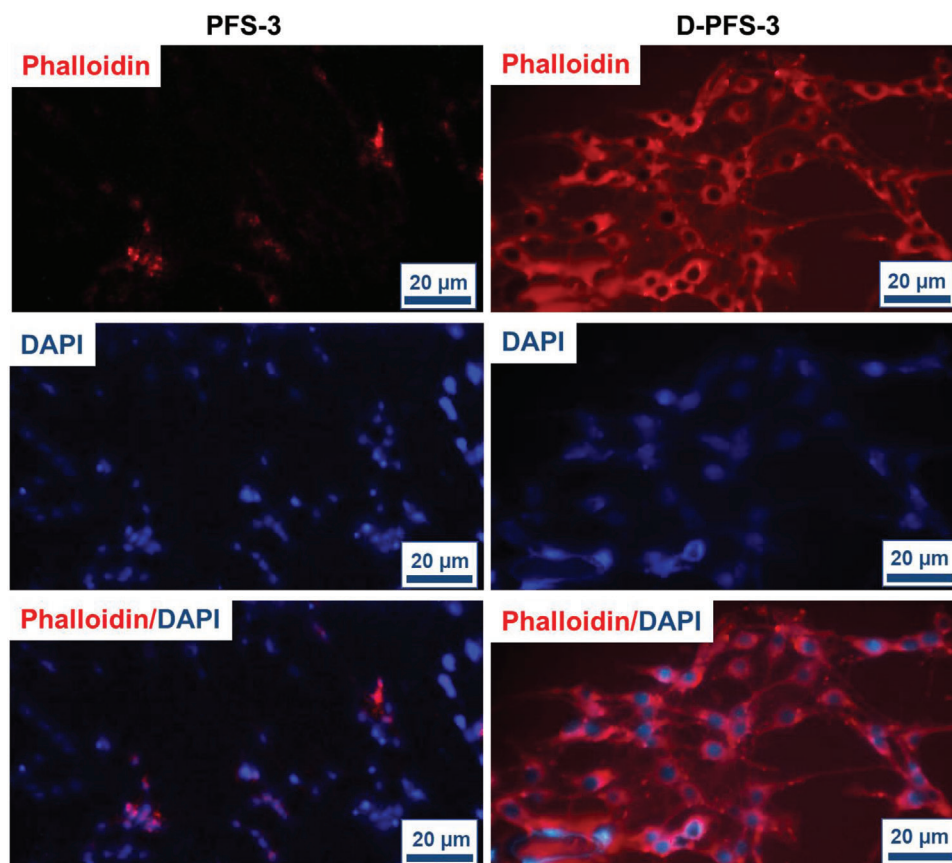
Figure 7. Morphology of stained proliferated HDF cells on scaffolds. Cell nuclei were stained with DAPI, F-actin stained with Alexa Fluor® 488-phalloidin (left: PFS-3; right: D-PFS-3).

it was possible to use water as cutting medium instead of harmful organic solvents, but for better dispersion of electrospun short fibers in water, application of surfactant was essential even with a rather low concentration, 0.01% in this work. The PFSs had physically cross-linked structure to maintain the structural integrity after thermal annealing step. PFS without any surface modification showed high hydrophobicity. In contrast, high hydrophilicity of PFS was achieved successfully by surfactant dip coating, which was scalable and fast. The treatment of the PFSs by surfactant resulted in thorough hydrophilization, which was obviously required for successful cell seeding. It was also obvious from our results, that cell seeding did occur inside the sponge within a short time (2 days). In contrast, the model studies showed that untreated PFS and plasma-treated PFS were hydrophobic inside, which was detrimental for cell seeding. The significantly increased high hydrophilicity of surface modified sponge was stable in aqueous state, and the hydrophilicity of PFS was favorable for cell growth, proliferation, and penetration, offering its potential application in fields like hard tissue engineering, and dental material. Fertilization is another potential application, because the hydrophilic sponge could serve as water reservoir for water management. The cell tests also indicated that surfactant dip coating did not harm the cells tested in this work during the test period. This could help to understand the effect of textile-based microplastic waste, such as short fibers, on cells as well.

However, this conclusion will need further verification with other scaffolds, fiber geometries, and polymers, which we will follow up in future work. Follow-up future work should surely also address the correlation of the porosity and pore size distribution of hydrophilized PLLA sponges on cell compatibility and cell proliferation.

4. Experimental Section

Materials: Chloroform (CHCl$_3$, VWR), dimethylformamide (DMF, Fisher Chemical), acetic acid (AA, Sigma-Aldrich), ethanol, (EtOH), polysorbate 20 (Tween 20, Acros, Fisher Scientific), poly(ϵ-caprolactone) (PCL, Capa 6800, Perstorp), poly (*L*-lactide) (PLLA, Ingeo Biopolymer PLLA 4043D, Nature-Works LLC) were used as received. Human dermal fibroblast (HDF) cells (Hu02) and human osteosarcoma cell line (MG63) cells were produced from Iranian Biological Resource Centre (IBRC, Tehran, Iran).

Characterization Methods: Molecular weight of the PLLA and PCL used for PFSs fabrication was characterized by gel permeation chromatography (GPC) equipped with a Styrene-divinylbenzene (SDV) precolumn (particle size 5 µm; PSS Mainz) and SDV linear XL column (particle size 5 µm, PSS Mainz). Samples were dissolved in CHCl$_3$ with a flow rate of 0.5 mL min^{-1} was used for measurements. The calibration was done with narrowly distributed polystyrene standards (PSS calibration kit). The results were shown in Figures S6 and S7 (Supporting Information). Differential scanning calorimetry (DSC, Netzsch, 204 F1, Phoenix) measurements were
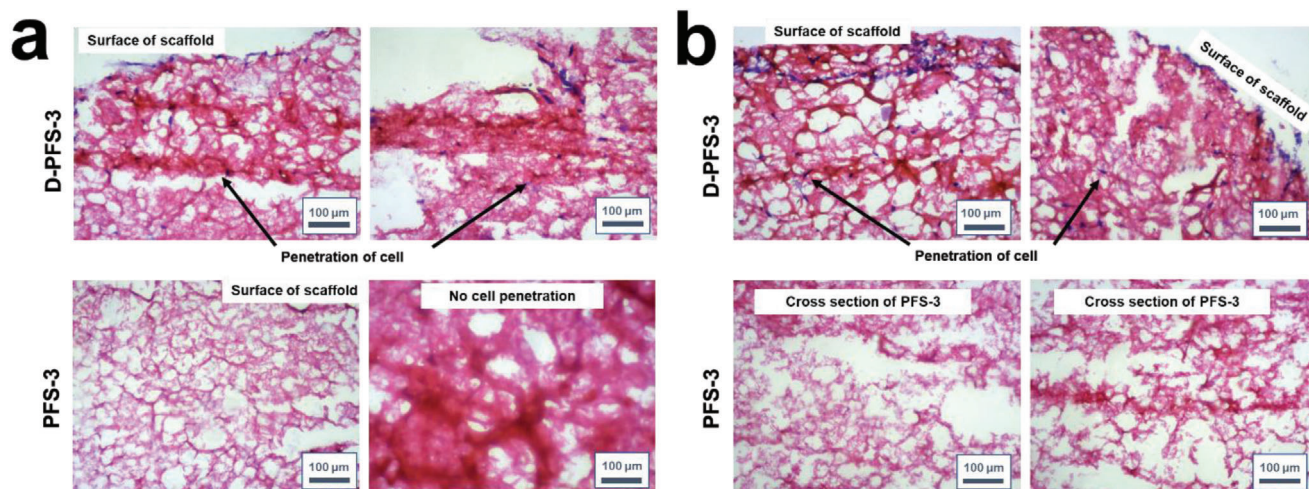
Figure 8. The representative images of H&E-stained histological sections of seeded a) MG63 cells and b) HDF cells on surface and cross section of PFSs after 48 h cultivation.

performed on raw polymer material at a heating rate of 10 K min^{-1}. Morphology of samples was imaged by scanning electron microscopy (SEM, LEO 1530, Zeiss). The samples were first sputter coated with Pt by sputter coater (208 HR from Cressington, Watford, England). Contact angle measurements were done by Drop Shape Analyzer (Krüss Advance, v.1.3.1) at room temperature, and the volume of deionized water drop was 4 μL. For hydrophilic dye staining method, the sponge samples were immersed into hydrophilic dye (Wusitta blau, Erich Wutzig) solution (as received from company) for 30 min at 22 °C. The coated sponges were then cut vertically to check if the internal part was stained by Wusitta blau.

Preparation of Electrospun Nonwoven: Electrospinning of PLLA/PCL was done following a previous publication with further modification.[53] In brief, 3.78 g PLLA (6.3 wt.%) and 0.42 g PCL (0.7 wt.%) were dissolved in a solvent mixture containing 39.06 g CHCl$_3$ (65.1 wt.%), 8.37 g AA (13.95 wt.%), and 8.37 g DMF (13.95 wt.%). This solution was filled in a plastic syringe (Injekt, 2 mL, B. Braun) assembled with a blunt-ended stainless steel needle (Sterican, Ø = 0.4 mm, B. Braun). The following conditions were applied for electrospinning: voltage 12.5 kV, flow rate 1.3 mL h^{-1}, and the distance between needle and collector 20 cm with relative humidity ≈20% and temperature ≈22 °C. The electrospun nonwoven was collected on a rotating cylinder (diameter 8.5 cm, length 21 cm, rotation speed 100 rpm) covered by slick parchment paper connected to −0.8 kV negative voltage.

Preparation of Short Fiber Dispersion: The electrospun nonwoven was stored under ambient conditions (101.3 MPa, 20 °C) for 12 h and cut into 2 × 2 cm^2 pieces. 1.5 g nonwoven was then cut into short fibers by a Gastroback kitchen mixer using ≈500 mL ice/water as cutting medium. Higher concentrations of short fiber suspension were reached by selective removal of water by filtration.

Preparation of PFSs: The short fibers were dispersed in aqueous solution with different concentrations of Tween 20 (0.01 wt.% or 1 wt.%). Taking polymer fiber-based sponge 3 (PFS-3) as an example, 0.01 g of Tween 20 was added into 100 g dispersion of short fiber, thus, the concentration of Tween 20 is 0.01 wt.% with respect to the dispersion (water as dispersion medium, approximate short fiber concentration 50 mg mL^{-1}), and the suspension was stirred vigorously by a Vortex-m shaker at 3000 rpm to realize homogeneity. 5 g of the suspension was then transferred into a cylindrical glass vial with diameter of 19 mm, frozen by immersion in EtOH bath at −30 °C for 15 min. The diameter of the glass vial and the amount of suspension added into the vial will together determine the dimension of the sponges. The frozen suspension was freeze-dried in Christ Beta-2-16 freeze-dryer at −70 °C, 0.1 mbar for 24 h. To achieve physical cross-linking, the dried product was put in oven to subject thermal annealing at 60 °C for 1 h under atmosphere pressure. PFSs with varied densities

were prepared by adjustment of the concentration of short fibers in the dispersion (Table 1). For example, in the case of sponges with lower density, 0.01% Tween 20 aqueous solution was added in the short fiber suspension to reach a lower concentration of the short fibers. Contrarily, for higher-density sponges, more of the dispersion medium, 0.01% Tween 20 aqueous solution was removed by filtration to get a higher concentration of the short fibers.

Dip Coating: The thermally annealed PFS-3 and PFS-2 were subsequently submerged in 1 wt.% Tween 20/H$_2$O solution for 30 min. After being taken out from Tween 20 solution, the PFS was dried in freeze-dryer for removal of water. The dip-coated sponge was named as D-PFS-3 and D-PFS-2, respectively.

Plasma Treatment: Plasma treatment was done by Air-Plasma oven (MiniFlecto-PC-MFC, Gala Instruments, v. 2.0.9, 2009). PFS-3 were treated under 0.5 mbar pressure with 100% air, the power was 20 W and the duration was 15 min. The plasma-treated sample was named as P-PFS-3.

In Vitro Cytocompatibility Assay (MTT Assay on Leachate Extracted from Samples): The possibility of releasing any toxic material from the prepared PFSs was checked out by applying MTT assay on the cells with existence of extracted leachates of immersed samples in the culture medium at different time intervals. To this aim the freshly synthesized samples were immersed in the culture medium for different time at 37 °C and then MTT assay was applied to cells cultured in the presence of the leachate. The standard culture medium was used as negative control. To check the leaking of any toxic material, the certain amount of standard culture medium with the extracted leachate from sponges at different time intervals was replaced and compared the cell viability with negative control that is standard culture medium with no extracted leachates from sponges. The percentage of relative cell viability was calculated according to Equation 1:

$$\text{cell viability\%} = \frac{OD_{sample}}{OD_{negative\ control}} \quad (1)$$

OD designates the optical density.

Adhesion of MG63 and Human Dermal Fibroblast (HDF) Cells on the PFSs: The following procedure was used to analysis the HDF and MG63 cells' relative adhesion and proliferation on the both D-PFS-3 and PFS-3 scaffolds. First, the scaffold specimens were cut in a suitable size (0.3 cm^2 basal area and 0.5 cm height) to cover the bottom of each well and then seeded with culture medium with density of 5× 10^4 cells mL^{-1}. After certain time intervals, the PFS/cells were removed and washed at least three times to remove the unattached cells from sample surfaces. The number of adhered cells was quantified by MTT assay. The standard calibration

ADVANCED SCIENCE NEWS

www.advancedsciencenews.com

{M} acro-olecular
Bioscience
www.mbs-journal.de

curve was plotted by applying MTT assay on an identified number of cells on a 96-well plate. Then, MTT assay was performed on each sample with adhered cells, and the number of attached cells was calculated from the standard calibration curve.

The number of adhered cells on the PFSs was quantified through the MTT assay on the PFS/cells construct. Then, the relative cell viability and relative cell adhesion percent were calculated by Equation 2.

$$\text{relative cell adhesion}\% = \frac{\text{OD}_{\text{sample}} - \text{OD}_{\text{positive control}}}{\text{OD}_{\text{negative control}}} \quad (2)$$

OD designates the optical density.

The standard tissue culture plate (TCP) was tested as a negative control, and the scaffolds with no cells were tested as a positive control.

Finally, the adhered cells were stained with DAPI/Phalloidin and imaged under a Confocal microscope for DAPI (359 nm) and Phalloidin (550 nm).

Cell Penetration Assay: The cell penetration depth into the PFSs samples was assessed by staining of penetrated cells and formed tissue via histological analyses. The constructed PFSs/cell samples (The PFSs/cell samples were prepared based on the procedure described in the previous section, the same cell number and same cell culture medium and incubation time) were separately fixed in 10% formalin and then dehydrated through graded alcohol series and fixed in paraffin wax. Serial sections of 5 μm thickness were cut via microtome and the grown cells and were stained with Hematoxylin and Eosin (H&E). These stained sections were observed under a microscope, and photomicrographs were captured. The depth of stained area that were the penetrated cells were analyzed by Image J software to evaluate the depth of cell growth and penetration into the PFS samples.

Statistical Analysis: The analysis of recorded data was performed with One-Way ANOVA with the Tukey post hoc test. The significance level was set at $p \leq 0.05$.

Supporting Information

Supporting Information is available from the Wiley Online Library or from the author.

Conflict of Interest

The authors declare no conflict of interest.

Data Availability Statement

The data that support the findings of this study are available in the supplementary material of this article.

[1] G. J. Christ, J. M. Saul, M. E. Furth, K.-E. Andersson, *Pharmacol. Rev.* **2013**, *65*, 1091.
[2] A. Joraku, C. A. Sullivan, J. J. Yoo, A. Atala, *Laryngoscope* **2005**, *115*, 244.
[3] S. D. Patil, D. G. Rhodes, D. J. Burgess, *AAPS J.* **2005**, *7*, E61.
[4] A. Nagarsekar, H. Ghandehari, *J. Drug Targeting* **1999**, *7*, 11.
[5] B. Amsden, A. Hatefi, D. Knight, E. Bravo-Grimaldo, *Biomacromolecules* **2004**, *5*, 637.
[6] O. Dechy-Cabaret, B. Martin-Vaca, D. Bourisssou, *Chem. Rev.* **2004**, *104*, 6147.
[7] M. Sander, *Environ. Sci. Technol.* **2019**, *53*, 2304.
[8] Z. Majeed, K. Ramli Nur, N. Mansor, Z. Man, *Rev. Chem. Eng.* **2015**, *31*, 69.
[9] J. M. Millican, S. Agarwal, *Macromolecules* **2021**, *54*, 4455.
[10] X.-F. Wei, M. Bohlén, C. Lindblad, M. Hedenqvist, A. Hakonen, *Water Res.* **2021**, *198*, 117123.
[11] A. Kumar, A. R. Weig, S. Agarwal, *Macromol. Mater. Eng.* **2022**, *307*, 2100602.
[12] W. Amass, A. Amass, B. Tighe, *Polym. Int.* **1998**, *47*, 89.
[13] I. Vroman, L. Tighzert, *Materials* **2009**, *2*, 307.
[14] X. Wang, B. Ding, B. Li, *Mater. Today* **2013**, *16*, 229.
[15] H. Amani, H. Arzaghi, M. Bayandori, A. S. Dezfuli, H. Pazoki-Toroudi, A. Shafiee, L. Moradi, *Adv. Mater. Interfaces* **2019**, *6*, 1900572.
[16] N. Yoon Sung, Y. Joon Jin, L. Jae Gwan, P. Tae Gwan, *J. Biomater. Sci., Polym. Ed.* **1999**, *10*, 1145.
[17] X. Garric, J.-P. Molès, H. Garreau, J.-J. Guilhou, M. Vert, *J. Biomed. Mater. Res.* **2005**, *72A*, 180.
[18] A. Zhu, M. Zhang, J. Wu, J. Shen, *Biomaterials* **2002**, *23*, 4657.
[19] Y. Wan, X. Qu, J. Lu, C. Zhu, L. Wan, J. Yang, J. Bei, S. Wang, *Biomaterials* **2004**, *25*, 4777.
[20] S. Sarapirom, L. D. Yu, D. Boonyawan, C. Chaiwong, *Appl. Surf. Sci.* **2014**, *310*, 42.
[21] Y.-P. Jiao, F.u-Z. Cui, *Biomed. Mater.* **2007**, *2*, R24.
[22] Y. Cheng, S. Deng, P. Chen, R. Ruan, *Front. Chem. China* **2009**, *4*, 259.
[23] T. Sritapunya, B. Kitiyanan, J. F. Scamehorn, B. P. Grady, S. Chavadej, *Colloids Surf., A* **2012**, *409*, 30.
[24] T. Ren, N. Xu, C. Cao, W. Yuan, X. Yu, J. Chen, J. Ren, *J. Biomater. Sci., Polym. Ed.* **2009**, *20*, 1369.
[25] A. G. Mikos, G. Sarakinos, S. M. Leite, J. P. Vacant, R. Langer, *Biomaterials* **1993**, *14*, 323.
[26] S.-J. Liu, C.-L. Hsueh, S. Wen-Neng Ueng, S.-S.u Lin, J.-K. Chen, *Asia-Pac. J. Chem. Eng.* **2009**, *4*, 154.
[27] I. O. Smith, X. H. Liu, L. A. Smith, P. X. Ma, *WIREs Nanomed. Nanobiotechnol.* **2009**, *1*, 226.
[28] Y. S. Nam, J. J. Yoon, T. G. Park, *J. Biomed. Mater. Res.* **2000**, *53*, 1.
[29] P. X. Ma, R. Zhang, *J. Biomed. Mater. Res.* **1999**, *46*, 60.
[30] W. Yu, X. Sun, H. Meng, B. Sun, P. Chen, X. Liu, K. Zhang, X. Yang, J. Peng, S. Lu, *Biomater. Sci.* **2017**, *5*, 1690.
[31] Y. Si, J. Yu, X. Tang, J. Ge, B. Ding, *Nat. Commun.* **2014**, *5*, 5802.
[32] G. Duan, S. Jiang, V. Jérôme, J. H. Wendorff, A. Fathi, J. Uhm, V. Altstädt, M. Herling, J. Breu, R. Freitag, S. Agarwal, A. Greiner, *Adv. Funct. Mater.* **2015**, *25*, 2850.
[33] S. Jiang, S. Agarwal, A. Greiner, *Angew. Chem., Int. Ed.* **2017**, *56*, 15520.
[34] F. Deuber, S. Mousavi, M. Hofer, C. Adlhart, *ChemistrySelect* **2016**, *1*, 5595.
[35] W. Chen, S. Chen, Y. Morsi, H. El-Hamshary, M. El-Newhy, C. Fan, X. Mo, *ACS Appl. Mater. Interfaces* **2016**, *8*, 24415.
[36] W. Chen, J. Ma, L. Zhu, Y. Morsi, H. EI-Hamshary, S. S. Al-Deyab, X. Mo, *Colloids Surf., B* **2016**, *142*, 165.
[37] T. Xu, J. M. Miszuk, Y. Zhao, H. Sun, H. Fong, *Adv. Healthcare Mater.* **2015**, *4*, 2238.
[38] T. Xu, Q. Yao, J. M. Miszuk, H. J. Sanyour, Z. Hong, H. Sun, H. Fong, *Colloids Surf., B* **2018**, *171*, 31.

[39] J. Miszuk, Z. Liang, J. Hu, H. Sanyour, Z. Hong, H. Fong, H. Sun, *ACS Appl. Bio Mater.* **2021**, *4*, 3639.

[40] M. Mader, V. Jérôme, R. Freitag, S. Agarwal, A. Greiner, *Biomacromolecules* **2018**, *19*, 1663.

[41] M. Mader, M. Helm, M. Lu, M. H. Stenzel, V. Jérôme, R. Freitag, S. Agarwal, A. Greiner, *Biomacromolecules* **2020**, *21*, 4094.

[42] J. Y. Cheong, M. Mafi, L. Benker, J. Zhu, M. Mader, C. Liang, H. Hou, S. Agarwal, I.l-D. Kim, A. Greiner, *ACS Appl. Mater. Interfaces* **2020**, *12*, 18002.

[43] R. S. Kurusu, N. R. Demarquette, *Eur. Polym. J.* **2017**, *89*, 129.

[44] R. Vasita, G. Mani, C. M. Agrawal, D. S. Katti, *Polymer* **2010**, *51*, 3706.

[45] J. Jensen, *Sci. Total Environ.* **1999**, *226*, 93.

[46] G. Wypych, in *Databook of Antistatics*, (Ed: G. Wypych), Elsevier, Oxford, UK **2014**, Ch. 3.1.

[47] H. Gholami, H. Yeganeh, R. Gharibi, M. Jalilian, M. Sorayya, *Polymer* **2015**, *62*, 94.

[48] N. Baheiraei, R. Gharibi, H. Yeganeh, M. Miragoli, N. Salvarani, E. Di Pasquale, G. Condorelli, *J. Biomed. Mater. Res. Part A* **2016**, *104*, 1570.

[49] A. Rezapour-Lactoee, H. Yeganeh, S. N. Ostad, R. Gharibi, Z. Mazaheri, J. Ai, *Mater. Sci. Eng., C* **2016**, *69*, 804.

[50] A. Meydani, S. Yousefi, R. Gharibi, S. Kazemi, M. B. Teimouri, *ChemistrySelect* **2019**, *4*, 3315.

[51] A. P. Periyasamy, A. Tehrani-Bagha, *Polym. Degrad. Stab.* **2022**, *199*, 109901.

[52] N. B. Haro-Mares, J. C. Meza-Contreras, F. A. López-Dellamary, A. Richaud, F. Méndez, B. G. Curiel-Olague, G. Buntkowsky, R. Manríquez-González, *Surf. Interfaces* **2022**, *35*, 102412.

[53] J. Zhu, A. Kumar, P. Hu, C. Habel, J. Breu, S. Agarwal, *Global Challenges* **2020**, *4*, 2000030.